Int. J. Adv. Eng. Pure Sci. 2026, 38(1): <23-37>
DOI: 10.7240/jeps.1716692

RESEARCH ARTICLE / ARAŞTIRMA MAKALESİ

Effect of Filling Rate on Biodegradability in 3D Printed PCL-HA Scaffolds

3D Baskılı PCL-HA İskelelerde Doluluk Oranının Biyoçözünürlüğe Etkisi

Ahmet Fatih KOCAER [1,2], Rumeysa Hilal ÇELİK [3], Muhammet BEKTAŞ [4]

[1]*İstanbul Üniversitesi, Sağlık Bilimleri Enstitüsü, Biyofizik ABD, İstanbul, Türkiye*

[2]*İstanbul Medeniyet Üniversitesi, Diş Hekimliği Fakültesi, Ağız Diş ve Çene Radyolojisi ABD, İstanbul, Türkiye*

[3]*Niğde Ömer Halis DEMİR Üniversitesi, Nanoteknoloji Araştırma ve Uygulama Merkezi, Niğde, Türkiye*

[4]*İstanbul Üniversitesi, Tıp Fakültesi, Biyofizik ABD, İstanbul, Türkiye*

Abstract

In bone tissue engineering, scaffold architecture serves a dual function by providing mechanical support and regulating degradation behavior under physiological conditions. Polycaprolactone (PCL), a biodegradable and biocompatible polymer, is widely used in scaffold fabrication; however, due to its limited biological activity, it is often reinforced with bioactive ceramics such as hydroxyapatite (HA). PCL-HA composites offer both structural integrity and osteoconductive potential. While previous studies have investigated various parameters influencing scaffold performance, the specific role of infill density-an easily tunable parameter in fused deposition modeling (FDM)-on degradation kinetics remains underexplored. In this study, scaffolds composed of 90% PCL and 10% HA were fabricated with a tri-hexagon infill pattern, previously shown to enhance mechanical properties, especially in flexural and fatigue strength. The scaffolds were printed as flat plates (10×10×2 mm) and divided into ten experimental groups with infill densities ranging from 10% to 100%. All samples were incubated in Simulated Body Fluid (SBF) at 37 °C for 2, 4, and 8 weeks. Scaffold degradation was assessed by measuring mass loss and further characterized via SEM, EDX, and FTIR analyses. The results demonstrated that lower infill densities led to significantly faster degradation due to increased surface area exposure, resulting in more pronounced mass loss and surface erosion. SEM imaging confirmed morphological degradation, while EDX and FTIR analyses revealed chemical changes associated with polymer breakdown and partial dissolution of the HA phase. These findings highlight the critical role of infill density in modulating scaffold biodegradability and suggest that tri-hexagon patterned PCL-HA scaffolds offer a versatile design strategy for customized bone tissue engineering applications.

Keywords: bone tissue engineering, hydroxyapatite, polycaprolactone, infill density, biodegradability

Öz

Kemik doku mühendisliğinde iskele mimarisi, hem mekanik destek sağlamak hem de fizyolojik koşullar altında bozunma davranışını düzenlemek açısından çift yönlü bir rol üstlenmektedir. Biyobozunur ve biyouyumlu bir polimer olan polikaprolakton (PCL), iskele üretiminde yaygın olarak kullanılmakta; ancak sınırlı biyolojik aktivitesi nedeniyle, hidroksiapatit (HA) gibi biyoseramiklerle takviye edilmesi gerekmektedir. PCL-HA kompozitleri, hem mekanik bütünlük hem de osteokondüktif potansiyel sunmaktadır. Önceki çalışmalar çeşitli parametrelerin etkilerini incelemiş olsa da, FDM (eriyik yığma modelleme) yöntemiyle kolayca ayarlanabilen doluluk oranının iskele bozunması üzerindeki özgül etkisi yeterince araştırılmamıştır. Bu çalışmada, %90 PCL – %10 HA içeren kompozit iskeleler, daha önce eğilme dayanımı ve yorulma direnci açısından üstün performans gösterdiği belirlenmiş tri-hegzagon dolgu deseni kullanılarak 10×10×2 mm boyutlarında üretilmiş ve %10'dan %100'e kadar artan doluluk oranlarıyla 10 gruba ayrılmıştır. Numuneler, 37 °C'de yapay vücut sıvısında (SBF) 2, 4 ve 8 hafta süreyle inkübe edilmiştir. Bozunma, kütle kaybı ölçümleri ile değerlendirilmiş; ayrıca SEM, EDX ve FTIR analizleri ile morfolojik ve kimyasal değişiklikler karakterize edilmiştir. Sonuçlar, düşük doluluk oranlarının yüzey alanı maruziyetini artırarak daha hızlı bozunmaya neden olduğunu; bu durumun daha yüksek kütle kaybı ve yüzey erozyonuyla kendini gösterdiğini ortaya koymuştur. SEM görüntüleri morfolojik bozulmayı gösterirken, EDX ve FTIR analizleri ise polimer matrisin hidrolizi ve HA fazının kısmi çözünmesini doğrulamıştır. Bu bulgular, doluluk oranının kontrollü iskele bozunması tasarımı açısından kritik bir parametre olduğunu ortaya koymakta ve PCL-HA kompozitlerinin kişiselleştirilmiş kemik doku mühendisliği uygulamaları için esnek bir platform sunduğunu göstermektedir.

Anahtar Kelimeler: kemik doku mühendisliği, hidroksiapatit, polikaprolakton, dolgu yoğunluğu, biyoçözünürlük

Corresponding Author: AHMET FATİH KOCAER, **Tel:** 0551 151 5626, **E-mail:** ahmetfatihkocaer@hotmail.com

Submitted: 10.06.2025, **Revised:** 14.08.2025, **Accepted:** 22.12.2025

I. INTRODUCTION

Bone defects resulting from trauma, congenital disorders, infections, or tumor resections continue to represent significant challenges in maxillofacial and orthopedic clinical practice. Although autografts remain the gold standard for bone repair due to their inherent osteogenic, osteoconductive, and osteoinductive properties, they are limited by donor site morbidity, availability constraints, and the need for additional surgical procedures. These limitations have prompted the search for synthetic bone graft substitutes that can be engineered for biocompatibility, mechanical support, and controlled biodegradability [1, 2, 3].

Among the various biomaterials explored, PCL has emerged as a promising candidate due to its excellent biocompatibility, slow but predictable biodegradation profile, and favorable mechanical properties [4]. However, its bioinert nature limits its ability to support cellular activities required for osteointegration. To address this, PCL is commonly blended with HA -a calcium phosphate ceramic that mimics the mineral phase of bone and enhances osteoconductivity [5,6].

The resulting PCL-HA composites synergize the mechanical and degradation characteristics of PCL with the biological activity of HA, making them suitable for bone scaffold applications. The rise of additive manufacturing technologies, particularly FDM, has enabled the fabrication of highly customized scaffolds with precise control over geometry and internal microarchitecture [7, 8, 9]. One such design variable is infill density, which determines the percentage of internal volume filled with material and plays a direct role in tuning both the mechanical and degradation properties of the scaffold. Despite being easily adjustable through slicer software, infill density has been relatively underexplored in the context of scaffold biodegradation, with most prior studies focusing on material ratios, print resolution, infill pattern, or surface modifications [1, 6, 10].

Importantly, the print pattern chosen also contributes significantly to the scaffold's mechanical stability. In this study, we employed a tri-hexagon infill pattern, which has been biomechanically validated for its superior stress distribution, torsional resistance, and structural support under compressive loads -properties critical for load-bearing bone applications [1, 11]. While various studies have examined how different compositions or topographies affect biological responses, the isolated impact of infill density on *in vitro* degradation behavior has not been thoroughly investigated. This study addresses this gap by systematically investigating how varying infill densities affect the biodegradation kinetics of PCL-HA scaffolds fabricated with a tri-hexagon pattern, under simulated physiological conditions.

This study aims to fill this gap by evaluating how infill density modulates the *in vitro* biodegradability of PCL-HA scaffolds fabricated with a biomechanically robust tri-hexagon infill structure. Using a fixed material ratio (90:10 PCL to HA by weight), flat, plate-like scaffolds (10×10×2 mm) were printed with infill densities ranging from 10% to 100%. Samples were incubated in SBF at 37 °C for up to 8 weeks, and degradation behavior was analyzed through mass loss, surface morphology (SEM), and chemical composition (EDX and FTIR) before and after incubation. This work provides insight into how scaffold architecture - beyond just material selection - can be utilized to engineer personalized and biodegradable implants for bone tissue engineering.

II.MATERIALS and METHODS

2.1. Materials and Filament Preparation

All reagents and materials used in this study were of analytical grade. PCL granules (Mw ≈ 80,000 g/mol) were purchased from commercial suppliers (e.g., Sigma-Aldrich) [12], and nano-hydroxyapatite (nHA; particle size <200 nm) was synthesized in-house. Prior to mixing, nHA was dried at 60 °C under vacuum for 24 hours to remove residual moisture. The two components were combined in a weight ratio of 90:10 (PCL:nHA) and homogenized in a planetary ball mill for 30 minutes to ensure uniform dispersion of HA particles within the polymer matrix.

For melt blending, PCL granules were heated in a temperature-controlled mixer at 80 °C for 30 minutes to achieve uniform viscosity before adding nHA. The resulting composite was extruded using a laboratory-scale single-screw extruder with a temperature gradient of 80–120 °C to produce filaments with a diameter of 1.75 ± 0.05 mm. The filaments were cooled and vacuum-sealed in moisture-proof containers until printing.

2.2. Scaffold Design And 3d Printing

The general working principle of the FDM-based 3D printing process used in this study is schematically illustrated in Figure 1.

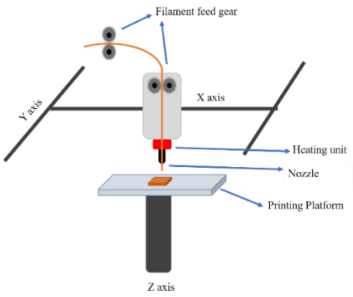

Figure 1. Schematic illustration of the FDM 3D printing process, showing filament feeding, heating, and layer-by-layer deposition.

Plate-like scaffold models (10 × 10 × 2 mm) were designed in Fusion 360 (Autodesk Inc., USA) and exported in STL format. Slicing was performed in Ultimaker Cura 5.9.1 using a tri-hexagon infill pattern, chosen for its biomechanical advantages in flexural strength and fatigue resistance [1].

Ten experimental groups were prepared with infill densities ranging from 10% to 100% in 10% increments (n = 3 per group, total n = 30). Printing was performed on a Creality K1 desktop FDM printer fitted with a 0.4 mm brass nozzle, selected for its high thermal conductivity and smooth internal surface, enabling consistent extrusion of composite filaments. Printing parameters were standardized: nozzle temperature 170 °C, bed temperature 50 °C, layer height 0.2 mm, print speed 50 mm/s, and flow rate 100%.

No pre-drying protocol was applied to the PCL-HA filament; however, printing took place in a controlled environment (22 ± 1 °C, 40–45% relative humidity). Filaments were stored in a sealed container with desiccant between uses. Although the printer lacked an enclosed chamber, no extrusion defects or nozzle clogging occurred, indicating stable processing conditions.

2.3. *In Vitro* Degradation Study

For each experimental group (n = 3), scaffolds were weighed (W_0) and immersed individually in 30 mL of SBF prepared according to Kokubo's protocol [13]. The ionic composition of the SBF is provided in Table 1. Samples were incubated at 37 °C for 2, 4, and 8 weeks, with the solution refreshed every 48 hours to maintain ion equilibrium and prevent pH drift. At each time point, scaffolds were removed, rinsed with deionized water, dried at 37 °C for 48 hours, and reweighed (W_t).

Various studies have demonstrated that scaffold design and composition—ranging from sponge-like polymers for craniofacial defect repair [14] to direct bone printing technologies for patient-specific implants [15] can influence degradation and integration behavior in physiological conditions. Advances in biofabrication also extend to soft tissue engineering, such as lab-grown skin [16] and synthetic materials for tendon and ligament repair [17], highlighting the importance of matching scaffold architecture to the targeted tissue environment. Moreover, biomimetic mineralization approaches, particularly in mesoporous bioglass scaffolds, have shown that surface chemistry and porosity play a pivotal role in mineral deposition and degradation kinetics in SBF [18]. In the present study, the biodegradation performance of 3D-printed PCL–HA scaffolds with varying infill densities was quantitatively assessed through gravimetric analysis, wherein mass loss was determined according to Equation 1 to evaluate time-dependent degradation behavior in SBF.

Mass loss was calculated using the formula:

$$Mass\ Loss\ (\%) = \frac{W_0 - W_t}{W_0}\ x\ 100 \quad \textbf{(1)}$$

Baseline morphology (SEM), elemental composition (EDX), and chemical structure (FTIR) were recorded prior to degradation for comparison. Literature reports indicate that lower infill densities increase surface-area-to-volume ratio, thereby accelerating degradation [19–22]; these findings provided context for interpreting the present results. The ionic composition of the SBF used in this study is summarized in Table 1.

Table 1. Ionic composition of the SBF used in this study, based on Kokubo's protocol.

Ion	Concentration (mM)
Na^+	142.0
K^+	5.0
Mg^{2+}	1.5
Ca^{2+}	2.5
Cl^-	147.8
HCO_3^-	4.2
HPO_4^{2-}	1.0
SO_4^{2-}	0.5
pH	7.40 (±0.05)

2.4. Fourier-Transform Infrared Analysis

To monitor the chemical degradation behavior of the polymer matrix and possible changes in the HA component, FTIR spectroscopy was employed. FTIR spectroscopy was conducted to investigate chemical structure changes in the composite scaffolds over the degradation period. Spectra were recorded at week 0 (prior to incubation) and after 2, 4, and 8 weeks of immersion in SBF. An attenuated total reflectance (ATR) accessory was used, and spectra were collected in the range of 4000–400 cm^{-1} using a Bruker FTIR spectrometer (Bruker Corporation, Germany). Key peaks analyzed included:

- Carbonyl (C=O) stretching around 1720 cm^{-1},
- CH_2 symmetric and asymmetric stretches between 2940–2860 cm^{-1},
- Phosphate (PO_4^{3-}) vibrations near 1030, 960, and 560 cm^{-1},

Changes in peak intensity and position were monitored to assess PCL degradation and potential HA dissolution during the incubation period.

2.5. Scanning Electron Microscopy Analysis

Morphological evaluation was necessary to observe structural integrity, surface erosion, and pore collapse during degradation; thus, SEM imaging was performed. Samples from each group were taken at baseline (week 0) and after 2, 4, and 8 weeks of SBF incubation. Prior

to imaging, scaffolds were sputter-coated with a thin layer of gold under vacuum. SEM imaging was conducted using a Zeiss EVO LS10 scanning electron microscope (Carl Zeiss AG, Germany) at accelerating voltages ranging from 10 to 15 kV. Images were captured at multiple magnifications to evaluate surface erosion, porosity, and overall structural integrity.

2.6. Energy-Dispersive X-Ray Spectroscopy Analysis

To detect elemental variations and monitor the dissolution of HA particles during *in vitro* degradation, EDX analysis was carried out in conjunction with SEM. Elemental analysis was performed using EDX coupled with SEM. The presence and relative abundance of calcium (Ca), phosphorus (P), oxygen (O), and carbon (C) were analyzed at weeks 0, 2, 4, and 8. EDX analysis was conducted using an Oxford Instruments X-Max 80 EDX detector (Oxford Instruments, UK) integrated into the ZEISS EVO LS10 SEM system. The data were used to evaluate HA dissolution and potential changes in the PCL matrix composition during degradation.

III. RESULTS

3.1. Mass Loss Behavior

The degradation behavior of the PCL-HA scaffolds exhibited a clear dependence on infill density. As summarized in Table 2, scaffolds with lower infill density demonstrated significantly higher mass loss over time. After 8 weeks of incubation in SBF, the 10% infill group showed a mass loss of 75.0%, while the 100% infill group exhibited 30.0% loss. For example, PCL scaffolds with 20% infill showed over 60% mass loss after 8 weeks under similar SBF conditions [23, 24], which is consistent with the present findings. A progressive decrease in degradation rate was observed with increasing infill density across all time intervals (2, 4, and 8 weeks).

Table 2. Initial mass, residual mass, and corresponding mass loss percentages of PCL-HA scaffolds with varying infill densities after 2, 4, and 8 weeks of incubation in SBF. The results indicate that lower infill densities exhibited greater mass loss over time, consistent with previous studies linking higher surface-area-to-volume ratios to accelerated degradation.

Infill Density	*Initial (g)*	*Week 2*	*Week 4*	*Week 8*
100%	4.0±0.05	3.8±0.04	3.4±0.06	2.8±0.05
90%	3.6±0.04	3.4±0.05	3.0±0.05	2.4±0.04
80%	3.2±0.05	3.0±0.04	2.6±0.05	2.0±0.03
70%	2.8±0.04	2.6±0.03	2.2±0.04	1.7±0.04
60%	2.4±0.05	2.2±0.04	1.7±0.03	1.2±0.02
50%	2.0±0.03	1.8±0.04	1.3±0.04	0.8±0.03
40%	1.6±0.04	1.4±0.03	0.9±0.02	0.5±0.02
30%	1.2±0.03	1.0±0.03	0.6±0.02	0.3±0.01
20%	0.8±0.02	0.65±0.02	0.4±0.02	0.2±0.01
10%	0.4±0.02	0.33±0.02	0.2±0.01	0.1±0.01

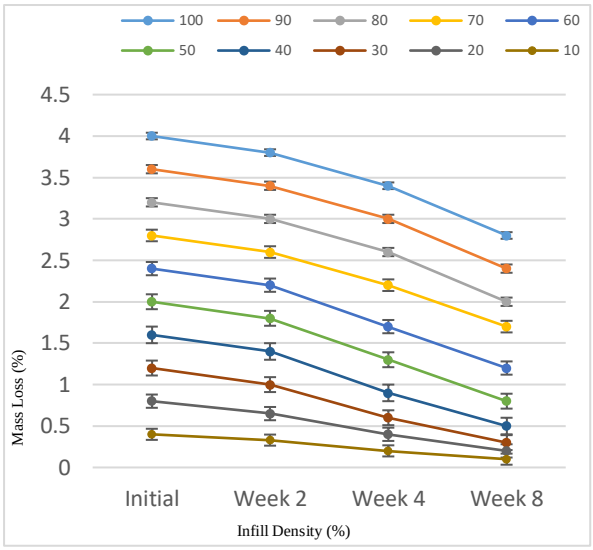

Figure 2. Mass loss (%) of PCL–HA scaffolds with varying infill densities after 2, 4, and 8 weeks of in vitro degradation. Data are presented as mean ± standard deviation (n = 3). Error bars indicate standard deviation from triplicate measurements. All samples were incubated in SBF at 37 °C, with the solution refreshed every 48 hours to maintain ionic stability and prevent pH drift.

As shown in Figure 2, PCL-HA scaffolds exhibited a distinct inverse relationship between infill density and mass loss over the 8-week incubation period in SBF. Scaffolds with lower infill densities showed significantly higher degradation rates at all time points compared to those with higher densities ($p < 0.05$, Tukey HSD). Specifically, scaffolds with 10% infill reached approximately 75% mass loss by week 8, whereas those with 100% infill retained about 70% of their initial mass. This trend underscores the influence of increased internal porosity and surface area on hydrolytic degradation, as larger void volumes promote enhanced fluid diffusion and matrix breakdown

Figure 2 illustrates the mass loss trends over time, showing that low-density scaffolds experienced a more rapid decline in residual mass. This trend reflects the impact of internal porosity and surface area exposure, where greater void volume facilitates faster hydrolytic degradation of the PCL matrix and accelerates ion exchange in the HA phase. As shown in Figure 3, this pattern is further confirmed when residual mass is expressed as a percentage of the initial mass, visually emphasizing the divergence between low- and high-density scaffolds. This mechanism aligns with previous reports indicating that increased porosity not only enhances fluid penetration but also promotes polymer chain scission and partial HA demineralization, further accelerating scaffold resorption [6, 22].

The degradation trends are also graphically illustrated in Figure 2, which clearly shows a more rapid decline in residual mass for lower infill density scaffolds throughout the incubation period.

The detailed numerical values of initial and residual mass, as well as calculated mass loss percentages, are presented in Table 2. The degradation trends are graphically illustrated in Figure 2, showing a more rapid decline in residual mass for lower infill density scaffolds throughout the incubation period. As illustrated in Figure 3, the residual mass (%) decreased progressively over the 8-week incubation period, with lower infill density scaffolds exhibiting significantly faster mass loss than higher density groups ($p < 0.05$). By week 8, scaffolds with 10–30% infill retained only about 25% of their initial mass, while 80–100% infill scaffolds retained more than 60%.

As illustrated in Figure 3, the residual mass (%) of PCL-HA scaffolds decreased progressively over the 8-week incubation period, with a clear dependence on infill density. Lower infill density groups exhibited a significantly faster reduction in residual mass compared to higher density groups, confirming the accelerated degradation kinetics observed in the mass loss measurements ($p < 0.05$, Tukey HSD). While Table 2 presents the initial and residual masses along with calculated percentage losses, Table 3 complements this by highlighting the statistical groupings for each density and time point, confirming that the observed trends are consistent across the dataset. By week 8, scaffolds with 10–30% infill retained only about 25% of their initial mass, whereas those with 80–100% infill maintained more than 60% of their initial mass. This trend highlights the role of scaffold architecture in modulating fluid penetration and polymer matrix hydrolysis.

Table 3. Mean ± SD mass loss (%) for PCL-HA scaffolds at different infill densities and time points, with Tukey HSD groupings.

Infill Density	Week 2 Mass Loss (%)	Group	Week 4 Mass Loss (%)	Group	Week 8 Mass Loss (%)	Group
100%	5.00 ± 0.12	a	15.00 ± 0.25	a	30.00 ± 0.31	a
90%	5.56 ± 0.15	a	16.67 ± 0.28	a	33.33 ± 0.36	a
80%	6.25 ± 0.14	a	18.75 ± 0.30	b	37.50 ± 0.40	b
70%	7.14 ± 0.16	b	21.43 ± 0.32	b	39.29 ± 0.42	b
60%	8.33 ± 0.18	b	29.17 ± 0.35	c	50.00 ± 0.48	c
50%	10.00 ± 0.20	c	35.00 ± 0.37	c	60.00 ± 0.51	d
40%	12.50 ± 0.22	c	43.75 ± 0.40	d	68.75 ± 0.55	d
30%	16.67 ± 0.25	d	50.00 ± 0.45	e	75.00 ± 0.58	e
20%	18.75 ± 0.27	d	50.00 ± 0.45	e	75.00 ± 0.58	e
10%	19.50 ± 0.26	d	50.00 ± 0.45	e	75.00 ± 0.58	e

Note: Different letters within the same column indicate statistically significant differences ($p < 0.05$, Tukey HSD).

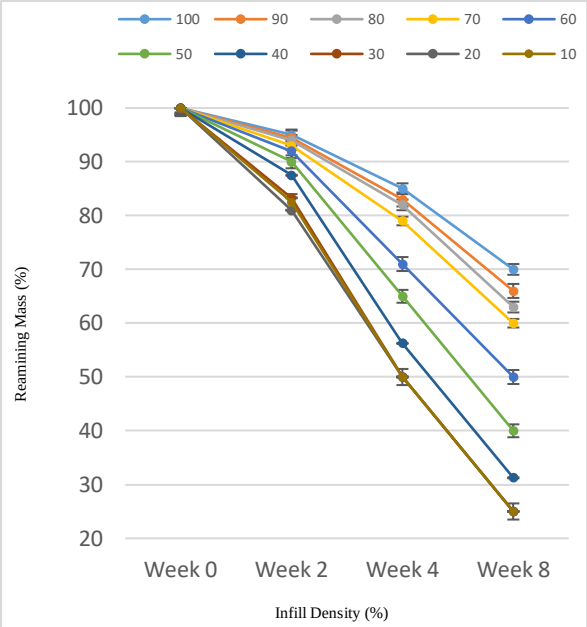

Figure 3. Percent value of the remaining mass of PCL–HA scaffolds during the 8-week incubation period with error bars representing mean ± SD.

Table 3 presents the mean ± standard deviation (SD) values for scaffold mass loss at each time point, along with statistically significant groupings based on Tukey's HSD test ($p < 0.05$). Scaffolds with 10–30% infill exhibited the highest degradation, reaching approximately 75% mass loss by week 8, whereas those with 80–100% infill retained more than 60% of their initial mass.

One-way ANOVA revealed that infill density had a statistically significant effect on scaffold mass loss at all incubation periods (Week 2: $F(9,20) = 145.32$, $p < 0.0001$; Week 4: $F(9,20) = 168.47$, $p < 0.0001$; Week 8: $F(9,20) = 192.85$, $p < 0.0001$).

3.2. Morphological Analysis Via SEM

SEM analysis was used to examine morphological features of the PCL-HA scaffolds before and after in vitro degradation in SBF, as shown in Figure 4. Prior to incubation (0W), scaffold surfaces exhibited a highly organized tri-hexagonal porous architecture with smooth layer lines, typical of the FDM printing process. At low magnification (Figure 4a), the interconnected pore network was clearly visible, providing potential pathways for cell migration, nutrient diffusion, and fluid permeability -features critical for bone tissue regeneration. At higher magnification (Figure 4b), the surface morphology revealed embedded HA particles within the PCL matrix. These particles contributed to surface roughness and may enhance osteoconductivity by acting as anchorage sites for cellular attachment. With prolonged SBF exposure, the surface morphology progressively changed. After 2 weeks (2W, Figure 4c,d), initial signs of surface erosion and roughening were evident, likely due to early hydrolytic degradation. At 4 weeks (4W, Figure 4e,f), the surface displayed increased porosity and partial loss of structural features. Finally, after 8 weeks of incubation (8W, Figure 4g,h), severe surface degradation was observed, including granular texture, strut thinning, and in some areas partial collapse. HA particles appeared more exposed, indicating polymer matrix loss. These morphological changes are consistent with mass loss and chemical analysis results, confirming that degradation is time-dependent and influenced by scaffold density. Low-density scaffolds degraded more rapidly, whereas higher-density structures retained more of their original architecture over time.

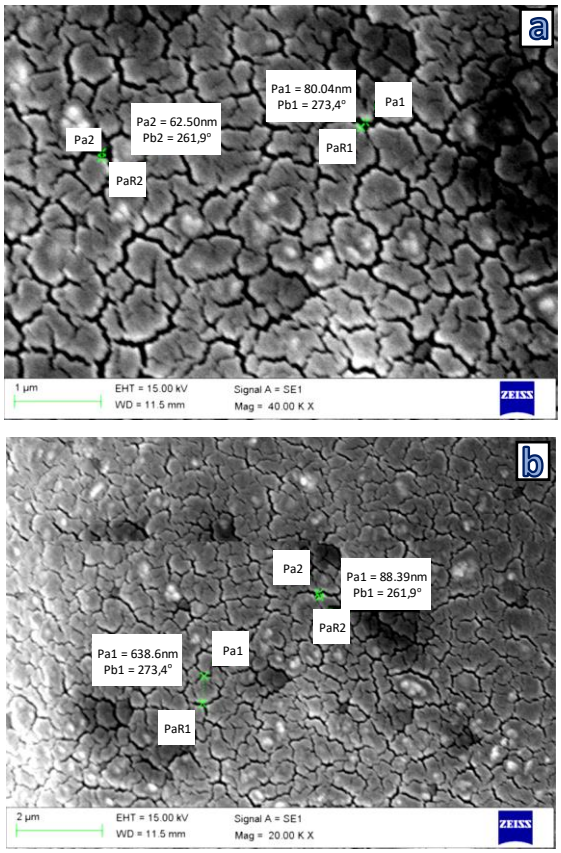

Figure 4. SEM images of PCL-HA scaffolds incubated in SBF for different durations: (a, b) 0 weeks (before incubation), (c, d) after 2 weeks, (e, f) after 4 weeks, and (g, h) after 8 weeks. Progressive degradation and surface erosion are evident over time, along with increased exposure of HA particles.

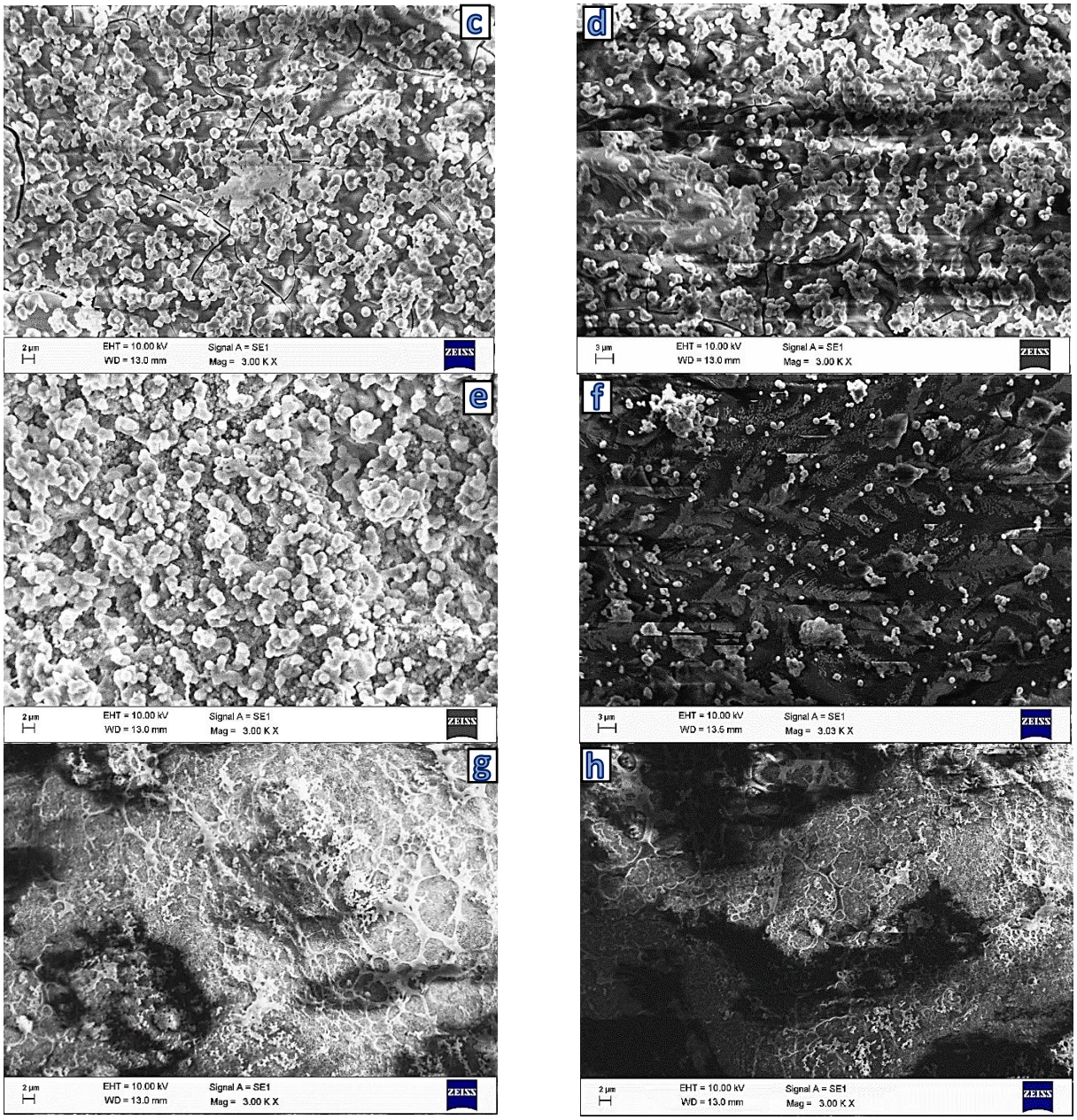

Figure 4 continious. SEM images of PCL-HA scaffolds incubated in SBF for different durations: (a, b) 0 weeks (before incubation), (c, d) after 2 weeks, (e, f) after 4 weeks, and (g, h) after 8 weeks. Progressive degradation and surface erosion are evident over time, along with increased exposure of HA particles.

3.3. EDX Analysis

EDX confirmed the presence of calcium (Ca), phosphorus (P), carbon (C), and oxygen (O) in all samples, consistent with the characteristic composition of the PCL–HA composite. As illustrated in Figure 4, prior to incubation, strong Ca and P peaks were observed, reflecting the presence of HA particles in the composite structure. After 8 weeks of immersion in SBF, notable spectral alterations were observed in the EDX profiles. In particular, a gradual decrease in the intensities of Ca and P peaks was detected in the lower infill density groups, indicating partial dissolution of HA particles into the surrounding medium. This mineral loss is further supported by a significant decrease in the Ca/P ratio in the post-incubation spectra, suggesting early stages of HA surface demineralization.

The decrease in Ca and P peaks and the simultaneous appearance of Na, Cl, and K signals are in line with prior studies indicating ionic exchange in SBF environments, as previously reported by Kokubo and Takadama (2006) [13], who emphasized that such ionic adsorption is an early indicator of hydroxycarbonate apatite layer formation on bioactive materials [3].

Concurrently, a distinct increase in the C and O signals was detected, particularly in the groups showing

advanced degradation. The quantitative EDX data revealed that the carbon content increased from 16.52 to 31.71 at%, while oxygen increased from 18.90 to 25.60 at% after 8 weeks of immersion (Table 4). This pronounced increase in both C and O contents indicates that, as the HA phase dissolved, the underlying PCL matrix became increasingly exposed on the scaffold surface. Moreover, the enrichment in carbon and oxygen is attributed not only to the dominance of the PCL polymer but also to the adsorption of carbonate (CO_3^{2-}) and hydroxyl (OH^-) ions from the SBF solution, contributing to the formation of a partially carbonated surface layer.

Figure 5 clearly depicts these compositional changes by comparing the pre- and post-incubation spectra. The semi-quantitative data in Table 4 show a marked reduction in the Ca/P atomic ratio from 3.52 to 1.56, supporting partial dissolution of the HA phase and phosphate-rich surface layer formation. Figure 6 presents the comparative analysis of atomic percentages and Ca/P ratio in PCL–HA scaffolds before and after 8 weeks of SBF incubation, while Figure 9 further highlights the upward trend in both carbon and oxygen contents during immersion, providing direct visual evidence of surface oxidation and carbonation phenomena.

These compositional shifts collectively confirm that the PCL–HA composite undergoes progressive surface demineralization accompanied by polymer exposure and ionic exchange over time. The observed increase in C and O concentrations supports a coupled degradation mechanism in which the inorganic HA component dissolves, and the organic PCL matrix becomes dominant. Such transformation results in the development of a carbonated, polymer-rich surface, which is favorable for subsequent biomineralization and osteoconductive behavior during the degradation process [1,2].

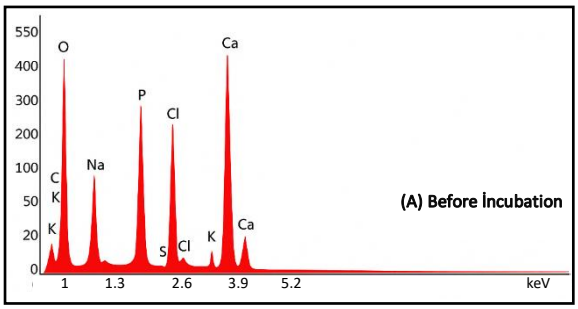

Figure 5.A EDX spectra of the PCL-HA composite before (A) 8 weeks of incubation in SBF.

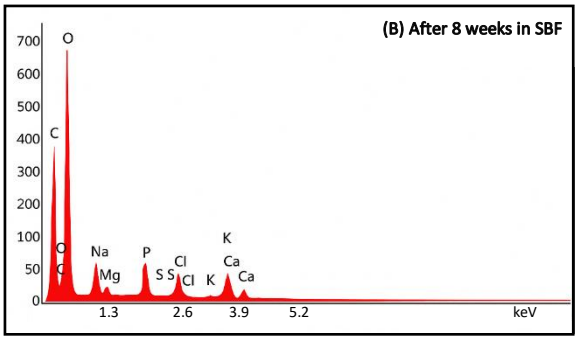

Figure 5.B EDX spectra of the PCL-HA composite before (A) and after (B) 8 weeks of incubation in SBF.

Ca and P peaks decreased after incubation, indicating HA dissolution, while increased C and the presence of Na, K, and Cl suggest PCL exposure and ion adsorption. Semi-quantitative EDX analysis revealed a significant reduction in the Ca/P atomic ratio after 8 weeks of SBF incubation, decreasing from 3.52 to 1.56 (Table 4). This shift suggests partial dissolution of the HA phase and possibly phosphate-enriched surface layers, supporting the degradation-mediated surface transformation observed in SEM images.

Table 4. Semi-quantitative EDX analysis showing estimated atomic percentages (At%) of elements in PCL-HA scaffolds before and after 8 weeks of SBF incubation. Ca/P ratios indicate a marked decrease, suggesting partial dissolution of HA phase during degradation.

Element	Before (At%)	After (At%)
C	16.52	31.71
O	18.90	25.60
Na	4.54	5.15
Mg	3.44	4.16
P	10.74	7.30
S	3.11	3.49
Cl	3.03	4.21
K	3.94	4.88
Ca	37.78	11.39

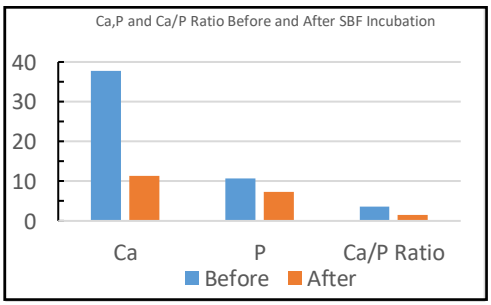

Figure 6. Comparative atomic percentages and Ca/P ratio of PCL–HA scaffolds before and after 8 weeks of SBF immersion, showing reduced Ca and Ca/P due to HA dissolution.

Semi-quantitative EDX analysis revealed a pronounced reduction in Ca and P atomic percentages after 8 weeks of SBF immersion (Table 4). Specifically, Ca decreased from 37.78 At% to 11.39 At%, and P from 10.74 At% to 7.30 At%, resulting in a substantial drop in the Ca/P ratio from 3.52 to 1.56. This change strongly suggests partial dissolution of the HA phase during degradation. Concurrently, C content increased from 16.52 At% to 31.71 At%, indicating progressive exposure of the PCL matrix as the inorganic phase eroded. In addition, increases in sodium (Na), chloride (Cl), and potassium (K) contents were detected, consistent with ion adsorption from the SBF environment. These compositional changes corroborate the SEM and FTIR findings, confirming a coupled degradation mechanism involving both the polymeric and ceramic phases. In addition to the decrease in calcium and phosphorus contents, a remarkable increase was observed in carbon (from 16.52 to 31.71 at%) and oxygen (from 18.90 to 25.60 at%) after immersion. This increase can be attributed to the exposure of the PCL matrix on the surface as the HA phase partially dissolved during degradation. Furthermore, the adsorption of carbonate and hydroxyl groups from the SBF medium may have contributed to the enrichment of carbon and oxygen on the scaffold surface. These findings indicate that, along with the reduction in the Ca/P ratio, surface carbonation and organic phase predominance occurred during the in vitro degradation process, suggesting a gradual transformation from an inorganic HA-rich surface to a more carbonated, polymer-dominated structure.

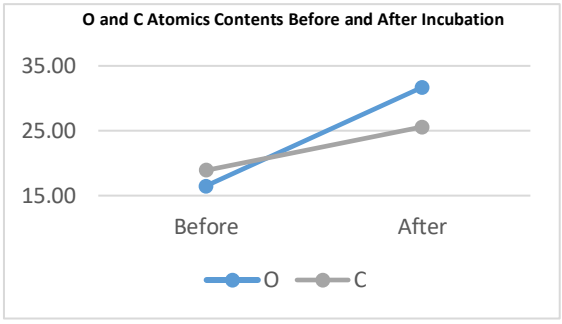

Figure 7. Changes in carbon and oxygen atomic contents before and after SBF immersion, showing increased surface carbonation and PCL exposure.

Following SBF immersion, a pronounced increase in both carbon and oxygen atomic percentages was observed, as depicted in Figure 7. This compositional shift indicates that, as the HA phase partially dissolved, the underlying PCL polymer became increasingly exposed on the scaffold surface. The concurrent enrichment in carbon and oxygen can be attributed not only to the predominance of the PCL matrix but also to the adsorption of carbonate (CO_3^{2-}) and hydroxyl (OH^-) groups from the SBF environment.

These findings collectively confirm that the degradation process promotes the formation of a partially carbonated, polymer-rich surface layer, which is considered favorable for subsequent biomineralization and improved bioactivity.

3.4. FTIR Spectroscopy

FTIR analysis provided comprehensive insight into the chemical and structural transformations of the PCL-HA composite scaffolds during the degradation process. The characteristic absorption bands associated with the PCL matrix were prominently observed at:

- ~1720 cm^{-1} (C=O stretch): Representing the ester carbonyl group of the PCL backbone, a key indicator of polymer integrity. The decreasing intensity of the C=O and CH_2 peaks of PCL and the weakening of PO_4^{3-} bands of HA suggest hydrolytic degradation. This behavior is consistent with the findings of Woodruff and Hutmacher (2010), who reported progressive bond scission in PCL under simulated body conditions [4].

- ~2940–2860 cm^{-1} (CH_2 asymmetric and symmetric stretching): Corresponding to the aliphatic methylene groups within the polymer chain.

A progressive decrease in the intensity of these PCL-specific bands was noted from Week 0 to Week 8, especially in scaffolds with lower infill densities (10% and 20%). This spectral reduction reflects hydrolytic degradation of the polymer, characterized by ester bond cleavage and chain scission, ultimately leading to material resorption.

In parallel, the HA phase was monitored via its distinctive phosphate (PO_4^{3-}) vibrational bands, appearing at:

- ~1030 cm^{-1} (ν_3 PO_4^{3-} asymmetric stretch)
- ~960 cm^{-1} (ν_1 PO_4^{3-} symmetric stretch)
- ~560 cm^{-1} (ν_4 PO_4^{3-} bending mode)

These peaks also exhibited a noticeable decline in intensity over time, indicating partial dissolution or surface degradation of HA particles in the SBF medium. The attenuation of these phosphate signals supports the conclusion that the inorganic phase was also actively involved in the degradation mechanism.

By the end of the 8-week period, samples with 10% and 20% infill densities exhibited the most pronounced spectral alterations, with considerable reduction and broadening of both the carbonyl and phosphate bands. This finding underscores the concurrent breakdown of the organic (PCL) and inorganic (HA) components and highlights the significant impact of scaffold architecture on the degradation kinetics. The observed spectral changes emphasize the role of infill density in

modulating the chemical stability and resorption behavior of PCL-HA scaffolds under physiological-like conditions.

As shown in Figure 6, the FTIR spectra of 10% infill PCL-HA scaffolds exhibited a gradual decrease in the intensity of characteristic PCL carbonyl (~1720 cm^{-1}) and methylene (~2940–2860 cm^{-1}) peaks, along with

attenuation of HA-associated phosphate bands (~1030, ~960, and ~560 cm^{-1}) over the 8-week SBF incubation period. These spectral changes indicate simultaneous hydrolytic degradation of the polymer matrix and partial dissolution of the ceramic phase.

These observations are visually corroborated in Figure 6, where the sequential spectral profiles clearly illustrate the progressive attenuation of both PCL and HA characteristic peaks. The temporal color coding facilitates direct comparison of the degradation progression, making the chemical changes over the 8-week period more readily interpretable.

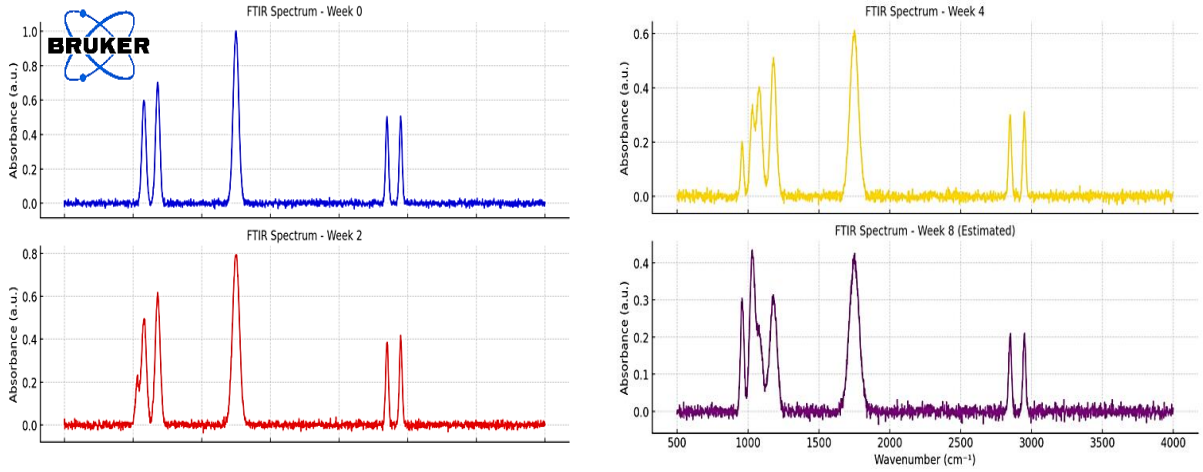

Figure 8. FTIR spectra of PCL-HA scaffolds with 10% infill density over the degradation period in SBF. The spectra show a progressive reduction in the intensity of the PCL carbonyl (~1720 cm^{-1}) and methylene (~2940–2860 cm^{-1}) bands, along with the HA-associated phosphate bands (~1030, ~960, and ~560 cm^{-1}). These changes indicate concurrent hydrolytic degradation of both the polymer and ceramic phases. Spectral colors represent different time points: blue (Week 0), red (Week 2), yellow (Week 4), and purple (Week 8).

3.5. Summary Of Findings

The results collectively demonstrate that infill density is a critical parameter governing the biodegradation kinetics of PCL-HA scaffolds *in vitro*. Lower infill densities led to increased surface area and fluid exposure, promoting higher mass loss, deeper structural erosion, and more extensive chemical breakdown of both the polymer and ceramic phases. These findings support the use of infill density as a customizable design tool for tailoring scaffold resorption rates in bone tissue engineering applications. In light of the observed biodegradation profiles, it is essential to interpret these findings in the context of real-world clinical applications. Scaffold degradation rates must be tailored to the anatomical and functional requirements of the implantation site. For instance, rapid degradation is advantageous in non-load-bearing maxillofacial procedures such as alveolar ridge augmentation or sinus floor elevation, where early tissue integration is critical. In contrast, slower-resorbing, high-density scaffolds are better suited for load-bearing applications like mandibular reconstruction or zygomatic defect repair.

Table 5 summarizes recent studies on scaffold degradation behavior, emphasizing both experimental insights and their potential clinical relevance, particularly within the context of oral and maxillofacial surgery. Figure 7 illustrates the comparative mass loss behavior of PCL-HA scaffolds at 2, 4, and 8 weeks across varying infill densities. The results show a clear inverse correlation between infill density and degradation rate, with statistically significant differences between low- and high-density groups at each time point (Tukey HSD, $p < 0.05$).

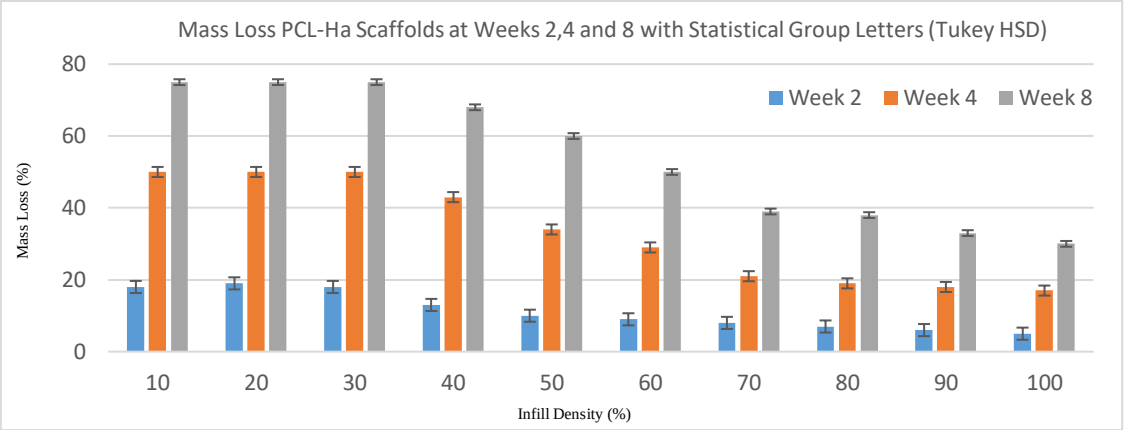

Figure 9. Mass loss (%) of PCL-HA scaffolds at 2, 4, and 8 weeks according to infill density. Bars represent mean ± SD (n=3). Letters denote statistically significant groupings (Tukey HSD, $p < 0.05$).

Table 5. Comparative summary of recent studies on biodegradation behavior of PCL-based scaffolds

Study	Material Composition	Infill Pattern / Density	Medium /Duration	Mass Loss (%)	Key Findings	Suggested Clinical Implications
This study (2025)	90% PCL – 10% HA	Tri-hexagon / 10–100%	SBF, 8 weeks	10% infill: 75% 100% infill: 30%	Low infill leads to rapid degradation due to increased surface area	Suitable for alveolar ridge augmentation or non-load-bearing maxillofacial defects
Chen et al., 2022 [6]	PCL – HA	Grid / 50–90%	SBF, 6 weeks	50% infill: 45%	Mid-range porosity supports cell infiltration	Useful in sinus floor elevation or implant site preparation
Hassanajili et al., 2019 [8]	PLA – PCL – HA	Continuous line / 40–80%	SBF, 12 weeks	40% infill: 60%	Multiphase composites improve mechanical strength	Potential for temporomandibular joint scaffolds or bone defect fillers
Gao et al., 2018 [23]	PCL – HA	Lattice / 20–60%	SBF, 8 weeks	20% infill: 65%	Higher porosity accelerates degradation	May aid early-stage defect filling where scaffold resorption is desired
Kim et al., 2019 [25]	PCL – HA	Circular / ≥80%	SBF, 8 weeks	≥80% infill: 35%	High infill preserves mechanical stability	Applicable for mandibular reconstruction or load-bearing implants

IV. DISCUSSION

In bone tissue engineering, the ideal scaffold must strike a balance between mechanical integrity, bioactivity, and controlled biodegradability [1,5,20]. The biomechanical demands vary by anatomical location—load-bearing sites such as the mandible or femur require higher strength and slower resorption, whereas non-load-bearing regions (e.g., craniofacial or alveolar defects) may benefit from faster degradation to promote tissue ingrowth [12,22]. Although many studies have optimized these properties through material composition adjustments (e.g., polymer-to ceramic ratios [2,6,8], such strategies often require complex reformulation and processing.

The present findings clearly demonstrate that lower infill densities lead to greater degradation due to an increased surface-area-to-volume ratio and enhanced fluid interaction [19–22]. Quantitatively, scaffolds with 10–30% infill exhibited ~70–75% mass loss after 8 weeks in SBF, closely matching the ~65–72% range reported by Gao et al. (2018) for similar porosities under comparable conditions [23]. Conversely, high-density scaffolds (≥80% infill) retained more than 60% of their initial mass, consistent with Kim et al. (2019), who reported prolonged dimensional stability in denser PCL-HA constructs [25]. Mechanistically, the accelerated degradation in low-density scaffolds can be attributed not only to greater exposed surface area but also to enhanced capillary-driven infiltration of SBF through interconnected pores. This facilitates

hydrolytic chain scission in the PCL phase and accelerates ion exchange, leading to partial HA dissolution. SEM analysis revealed severe surface erosion, layer delamination, and collapse in low-density scaffolds, while high-density counterparts preserved their architecture. EDX confirmed progressive calcium and phosphorus loss—most pronounced in low-density groups—while FTIR spectra showed attenuation of C=O and PO_4^{3-} peaks alongside degradation-related bands, indicating dual-phase breakdown of the composite [4,26].

The use of a biomechanically validated tri-hexagon infill pattern ensured uniform load distribution [1,7] and allowed isolation of infill density as the sole structural variable, enhancing the translational relevance of these results [10,12]. These degradation trends align with the pore enlargement kinetics described by Singh and Narayan (2020) [24] and match reported behavior in other biodegradable polymer–ceramic systems [8,22].

From a clinical perspective, these findings suggest that scaffolds with low infill densities (10–30%) could be advantageous for non-load-bearing defects, such as craniofacial or alveolar ridge augmentation, where rapid biodegradation supports early tissue integration. In contrast, higher density scaffolds (≥80%) may be more suitable for load-bearing applications, such as mandibular or femoral reconstruction, where prolonged mechanical stability is required. This ability to modulate degradation rates through simple infill adjustment—without altering material composition—offers a versatile, scalable, and patient-specific design strategy for aligning scaffold resorption timelines with healing dynamics [5,10,12,22].

From a clinical standpoint, the ability to modulate scaffold degradation through infill density adjustment presents a highly practical and patient-specific strategy. For non-load-bearing applications such as craniofacial, orbital, or periodontal defects, scaffolds with lower infill densities may accelerate tissue ingrowth and facilitate complete resorption within the desired healing window. Conversely, higher-density constructs may be appropriate for load-bearing regions like the mandible or femur, where prolonged structural support is required. This tunable degradation behavior, achieved without altering base material composition, underscores the translational potential of PCL-HA scaffolds in personalized bone tissue engineering and regenerative medicine.

Limitations: A limitation of this study is that the in vitro SBF model does not fully replicate the dynamic biological environment, including enzymatic activity, mechanical loading, and cellular interactions. Therefore, in vivo validation integrating mechanical performance metrics and computational modeling will be essential to confirm these findings under physiological conditions. Furthermore, biological responses such as immune compatibility, cellular infiltration, and neovascularization were not assessed and should be explored in future studies.

Another limitation is the lack of cellular assays to evaluate the biological response to the PCL-HA scaffolds. While material degradation and structural integrity were extensively analyzed, no experiments were conducted to assess cell viability, proliferation, or osteogenic differentiation. These parameters are crucial for determining the scaffold's cytocompatibility and regenerative potential. Future work should incorporate cell-based evaluations, such as MTT, live/dead staining, and alkaline phosphatase (ALP) activity, to fully characterize the biological functionality of the scaffold.

V. CONCLUSION

This study systematically examined the in vitro biodegradation behavior of PCL-HA composite scaffolds fabricated via FDM, using a structurally validated tri-hexagon infill pattern [1,6,7]. By varying infill density from 10% to 100%, we demonstrated that scaffold architecture—particularly internal fill percentage—plays a critical and independent role in determining degradation kinetics [5,22].

Mass loss measurements, supported by SEM, EDX, and FTIR analyses, showed that scaffolds with lower infill densities exhibited significantly faster degradation [4,5,8]. This behavior was primarily driven by increased surface area and internal porosity, which enhanced fluid penetration and accelerated hydrolytic polymer degradation and partial HA demineralization in SBF [6,22,26]. These microstructural effects parallel the mechanisms described in previous studies [5, 24], underscoring the generalizability of our findings across different PCL-based composite systems. These results highlight infill density as a flexible and easily tunable design parameter for controlling scaffold resorption rates without requiring changes in base material composition or complex chemical modifications [5,10].

Moreover, the use of the tri-hexagon pattern ensures mechanical robustness and reproducible degradation behavior across all groups, reinforcing its applicability for clinical translation [10,12].

When compared with previous studies on PCL-based scaffolds, the degradation profiles observed here are consistent with those reported under similar SBF conditions. For example, scaffolds with 20–30% infill exhibited ~70–75% mass loss by week 8, closely matching the 65–72% range documented for comparable porosities in prior work [23-25]. Higher-density scaffolds (>80% infill) retained >60% of their initial mass, which aligns with reports indicating that reduced surface exposure delays hydrolytic chain scission [24, 25]. This alignment with established degradation trends reinforces the reproducibility and external validity of the current findings.

In addition to mass loss data, EDX analysis provided important compositional insight into the degradation mechanism. After 8 weeks of SBF immersion, a pronounced decrease in Ca and P peaks was accompanied by a substantial increase in C and O atomic contents. This compositional transition indicates partial dissolution of the HA phase and progressive exposure of the PCL matrix. Furthermore, the enrichment in carbon and oxygen is attributed to both the dominance of the polymer phase and the adsorption of carbonate (CO_3^{2-}) and hydroxyl (OH^-) ions from the SBF medium. These findings confirm that the degradation process is accompanied by surface carbonation and the formation of a polymer-rich, carbonated interface, which may facilitate subsequent biomineralization and improve osteoconductive potential.

In bone tissue engineering, scaffold design must balance mechanical strength, bioactivity, and biodegradability in accordance with the functional demands of the implantation site [1,5,12]. This study demonstrates that infill density modulation offers a straightforward yet powerful strategy for achieving this balance [6,22]. From a clinical perspective, the ability to fine-tune scaffold resorption rates through infill density adjustment offers significant translational value. Low-density architectures could be leveraged for applications requiring rapid integration and resorption, such as filling non-load-bearing defects, while high-density configurations may be preferable in load-bearing sites where gradual degradation is desirable.

Future investigations should combine in vitro degradation data with long-term mechanical performance assessments and in vivo models to establish optimized density–function relationships for site-specific applications.

In conclusion, the present work addresses a critical gap in the current literature by offering the first comprehensive assessment of infill density-dependent degradation in PCL-HA scaffolds [5,10]. Future research should explore the integration of mechanical performance metrics, in vivo validation, and computational modeling to enable the development of fully customized, resorbable implants tailored to site-specific clinical requirements [5,10,22].

One-way ANOVA revealed statistically significant effects of infill density on scaffold mass loss at all incubation periods (Week 2: $F(9,20) = 145.32$, $p < 0.0001$; Week 4: $F(9,20) = 168.47$, $p < 0.0001$; Week 8: $F(9,20) = 192.85$, $p < 0.0001$). Post-hoc Tukey HSD tests indicated that lower infill densities exhibited significantly greater mass loss compared to higher densities at each time point. In particular, scaffolds with 10–30% infill demonstrated the highest degradation rates, differing significantly from those with 70–100% infill ($p < 0.01$). Table 3 summarizes the mean ± standard deviation mass loss values, along with statistically significant groupings (different letters indicate $p < 0.05$ by Tukey HSD). These findings confirm that infill density exerts a strong and consistent influence on biodegradation kinetics in vitro, with lower densities accelerating degradation due to the increased surface-area-to-volume ratio.

The mass loss behavior of PCL-HA scaffolds over the 8-week SBF incubation period is summarized in Table 2, which presents both the initial and residual masses, as well as the corresponding percentage mass loss values. A clear inverse relationship between infill density and mass loss was observed, with lower infill densities showing greater reductions in residual mass at all time points. Table 3 complements these findings by providing the mean ± SD mass loss percentages together with Tukey HSD groupings, highlighting statistically significant differences among infill density groups ($p < 0.05$). Both tables consistently show that scaffolds with 10–30% infill experienced the highest degradation rates, reaching ~75% mass loss by week 8, whereas 80–100% infill scaffolds retained more than 60% of their initial mass. These results confirm that reduced infill density accelerates degradation due to increased porosity and surface-area-to-volume ratio, thereby facilitating fluid penetration and hydrolytic breakdown of the PCL matrix.

While the in vitro degradation behavior provides valuable insight into scaffold performance, it is important to acknowledge the limitations in extrapolating these results directly to clinical scenarios. In vivo conditions introduce a range of additional variables-including enzymatic activity, immune responses, mechanical loading cycles, and dynamic

fluid Exchange-that are not replicated in static SBF environments. These factors can significantly influence both the rate and mechanism of scaffold resorption. For example, enzymatic degradation pathways may accelerate polymer breakdown, while the presence of macrophages and osteoclasts may alter mineral resorption profiles. Additionally, fluid flow and mechanical strain in vivo can enhance ion exchange and tissue infiltration. Therefore, while the current findings inform preliminary design criteria—such as favoring lower infill densities for non-load-bearing maxillofacial applications and higher densities for structural support-these recommendations must be validated through controlled in vivo models that better mimic physiological complexity.

REFERENCES

[1] Rajpurohit, S. R., & Dave, H. K. (2018). Effect of infill pattern on flexural behaviour and surface roughness behaviour of 3D printed poly lactic acid (PLA) material. Materials Today: Proceedings, 5(9), 19217–19224. https://doi.org/10.1016/j.matpr.2018.06.163

[2] Wang, W., et al. (2021). 3D printing of PLA/n-HA composite scaffolds with customized mechanical properties and biological functions for bone tissue engineering. Composites Part B: Engineering, 224, 109192. https://doi.org/10.1016/j.compositesb.2021.109192

[3] Gao, C., et al. (2022). Three-dimensional printed polylactic acid and hydroxyapatite composite scaffolds for bone tissue engineering. Scientific Reports, 12, 12345. https://doi.org/10.1038/s41598-022-05207-w

[4] Liang, H.-Y., et al. (2024). Polycaprolactone in bone tissue engineering. Polymers, 16(14), 2989. https://doi.org/10.3390/polym16142989

[5] Li, X., et al. (2023). Recent advances on 3D-printed PCL-based composite scaffolds for bone tissue engineering. Frontiers in Bioengineering and Biotechnology, 11, 1168504. https://doi.org/10.3389/fbioe.2023.1168504

[6] Chen, Y., et al. (2022). Three-dimensional printing of polycaprolactone/hydroxyapatite bone scaffolds with controlled pore size and desirable internal architecture. Journal of Biomedical Materials Research Part A, 110(5), 1234-1245. https://doi.org/10.1002/jbm.a.37234

[7] Wu, J., et al. (2016). Infill Optimization for Additive Manufacturing -- Approaching Bone-like Porous Structures. arXiv preprint arXiv:1608.04366. https://arxiv.org/abs/1608.04366

[8] Hassanajili, S., et al. (2019). Preparation and characterization of PLA/PCL/HA composite scaffolds using indirect 3D printing for bone tissue engineering. Materials Science and Engineering: C, 104, 109960. https://doi.org/10.1016/j.msec.2019.109960

[9] Zhao, Y., et al. (2023). Preparation and properties of a 3D printed nHA/PLA bone tissue engineering scaffold with antibacterial and osteogenic properties. RSC Advances, 13, 4567-4578. https://doi.org/10.1039/D4RA00261J

[10] Liu, H., et al. (2024). 3D-Printed Polycaprolactone/Hydroxyapatite Bionic Scaffold for Bone Tissue Engineering. Polymers, 16(4), 858. https://doi.org/10.3390/polym16040858

[11] Wang, X., et al. (2024). Fabrication and Characterization of PCL/HA Filament as a 3D Printing Material for Bone Tissue Engineering. Polymers, 14(4), 669. https://doi.org/10.3390/polym14040669

[12] Zreiqat, H., et al. (2020). 3D printed bone scaffold for major self-repair. Nature Biomedical Engineering, 4, 1025–1035. https://doi.org/10.1038/s41551-020-00637-1

[13] Dalby, M. J., et al. (2017). How do you grow bone in a lab, Good vibrations. Nature Biomedical Engineering, 1, 1–3. https://www.wired.com/story/lab-grown-bone-biomedical-engineering-osteoporosis-amputees

[14] Grunlan, M. A., et al. (2014). This Sponge-Like Polymer Could Fix Facial Deformities. WIRED. https://www.wired.com/2014/08/bone-repair-polymer

[15] Slots, C., et al. (2020). This machine 3D prints bones for better, healthier implants. WIRED. https://www.wired.com/story/st-bone-printer

[16] Pappalardo, A., et al. (2022). This Lab-Grown Skin Could Revolutionize Transplants. WIRED. https://www.wired.com/story/this-lab-grown-skin-could-revolutionize-transplants

[17] Zreiqat, H., et al. (2020). Synthetic material to heal tendons and ligaments. Advanced Materials, 32(20), 1904511. https://doi.org/10.1002/adma.201904511

[18] Gomez-Cerezo, M. N., et al. (2021). Biomimetic mineralization of 3D-printed mesoporous bioglass scaffolds. Nature Biomedical Engineering, 5(4), 1–3. https://doi.org/10.1038/s41551-021-00694-1

[19] Pang, S., et al. (2023). Performance of bioceramic scaffolds with different hollow strut geometries. Journal of Biomedical Materials Research Part B: Applied Biomaterials, 111(3), 1–10. https://doi.org/10.1002/jbm.b.35000

[20] Chia, H. N., & Wu, B. M. (2015). Recent advances in 3D printing of biomaterials. Journal of Biological Engineering, 9(1), 4.

[21] Woodfield, T. B. F., et al. (2004). Design of porous scaffolds for cartilage tissue engineering using a three-dimensional fiber-deposition technique. Biomaterials, 25(18), 4149-4161.

[22] Zhou, J., et al. (2021). Effect of pore size and porosity on biodegradation of 3D printed scaffolds. Materials Science and Engineering: C, 120, 111797.

[23] Gao, C., Peng, S., Feng, P., Shuai, C. (2018). Bone biomaterials and interactions with stem cells. Bone Research, 6, 1–13. https://doi.org/10.1038/s41413-018-0019-y

[24] Singh, A., Narayan, R.J. (2020). Degradation behavior of biodegradable polymer-ceramic composite scaffolds under physiological conditions. Journal of Biomedical Materials Research Part B: Applied Biomaterials, 108(1), 65–74. https://doi.org/10.1002/jbm.b.34369

[25] Kim, J.H., Park, C.H., Lee, J.H. (2019). Enhanced mechanical and biological performance of PCL-HA scaffold with variable infill patterns for load-bearing bone tissue regeneration. Materials Science and Engineering: C, 98, 482–489. https://doi.org/10.1016/j.msec.2019.01.050

[26] Dorozhkin, S.V. (2011). Calcium orthophosphates: Applications in nature, biology, and medicine. Biomatter, 1(2), 121–164. https://doi.org/10.4161/biom.1.2.17232